01 Jan 2001

Robust Control of Input Limited Smart Structural Systems

Sridhar Sana

Vittal S. Rao

Missouri University of Science and Technology

Robust Control of Input Limited Smart Structural Systems

Sridhar Sana and Vittal S. Rao

***Abstract*—Integration of controllers with smart structural systems require the controllers to consume less power and to be small in hardware size. These requirements pose as limits on the control input and the order of the controllers. Use of reduced order model of the plant in the controller design can cause spill over problems in the closed-loop system due to possible excitation of the unmodeled dynamics. In this paper, we present a method to design output feedback robust controllers for smart structures in the presence of control input limits considering unmodeled dynamics as additive uncertainty in the design. The performance requirements for the design are specified as regional pole placement constraints on the closed-loop poles. The controller design problem requires the maximization of damping ratio in the presence of additive uncertainty and control input limits. The resulting optimization problem for the controller design is formulated as a generalized eigenvalue problem involving linear matrix inequality (LMI) constraints. The proposed controller is designed and implemented on a multiinput–multioutput 3-mass smart structural test article. The tradeoffs involved in the controller design are analyzed and the performance and robustness specifications are verified experimentally.**

***Index Terms*—Actuator limits, linear matrix inequalities, robust control and regional pole placement, smart structures, spill over.**

I. Introduction

SMART structures research has found many applications in areas such as aerospace, automotive, and civil engineering due to the effective integration of sensors, actuators, signal processing, and control with structural systems to achieve good performance and adaptability to the environmental changes. There are several requirements on the controllers used in this integration such as simplicity of hardware, reduced bandwidth, and less power consumption. These requirements translate to constraints on the actuator force and the complexity of the controllers, respectively. Usually, a truncated or reduced order model is used in the controller design to achieve lower order controllers. But, the resulting unmodeled dynamics when excited can degrade the performance or lead to instability of the closed-loop system. This phenomenon is known commonly as *spill-over effect* in the structural control literature [1]. One of the approaches to alleviate this problem is to design robust controllers treating the unmodeled dynamics as uncertainty. Similarly the constraints on the control input will require tradeoffs in the performance and robustness that can be achieved by the control systems. This makes it important to include the control input constraints in the design phase itself. Also, the performance requirements of structural systems are usually specified in terms of the damping or decay rate requirements on the closed-loop system. These requirements can in turn be specified as regional constraints on the closed-loop pole locations. All the above dissimilar requirements on the controller design show the need for a multiobjective design procedure for the smart structures. Recently, linear matrix inequalities (LMIs) have been shown to be able to easily formulate such multiobjective design problems [2], [8]. Due to the recent advances in convex optimization like the development of interior point methods [5], and the availability of user friendly packages like LMI-toolbox [4] it has been possible to solve these LMI problems successfully. In this paper, we utilize LMIs to formulate and solve the controller design problem for the smart structures. This paper is a continuation of our work presented at a conference on smart structures [7]. The design procedure is applied on a 3-mass smart structural test article and the experimental results are included.

Manuscript received June 15, 2000; revised September 1, 2000. Recommended by Guest Editors S. O. R. Moheimani and G. C. Goodwin. This work was supported by the National Science Foundation under Grant EEC-9872392.

S. Sana is with the Department of Electrical and Computer Engineering, University of Missouri, Rolla MO 65401 USA (e-mail: sridhars@umr.edu).

V. S. Rao is with the Intelligent Systems Center, University of Missouri, Rolla MO 65401 USA (e-mail: raov@umr.edu).

Publisher Item Identifier S 1063-6536(01)00422-5.

II. Problem Formulation

A. Uncertainty Representation

In this section, we formulate the uncertainty representation to be used in the robust controller design for smart structures to eliminate spill-over problems. The unmodeled dynamics are formulated as additive unstructured uncertainty as shown in Fig. 1(a). Here G_{nom} is the nominal plant model containing the controlled modes of the structural system, $\Delta_{\text{additive}} \in RH_\infty$ is the linear time invariant (LTI) additive uncertainty representation in the nominal plant and W is a MIMO (multiinput–multioutput) LTI system chosen to normalize the uncertainty representation and satisfies the following constraint:

$$||\Delta_{\text{additive}}||_\infty \leq ||\Delta W||_\infty \tag{1}$$

where Δ is the normalized LTI uncertainty such that

$$||\Delta||_\infty \leq 1 \tag{2}$$

and C is a strictly proper output feedback controller with the same order as that of the generalized plant. The strictly proper controller is selected to guarantee the well posedness of the closed-loop system when the plant model has a nonzero D-matrix, which is typical for structural systems. Also, having the strictly proper controller simplifies the analysis and digital implementation. The state-space realization of the controller is given below

$$\begin{aligned} \dot{x}_c &= A_c x_c + B_c y \\ u &= C_c x_c. \end{aligned} \tag{3}$$

The corresponding linear fractional representation (LFR) is shown in Fig. 1(b). Here, P is known as the generalized plant

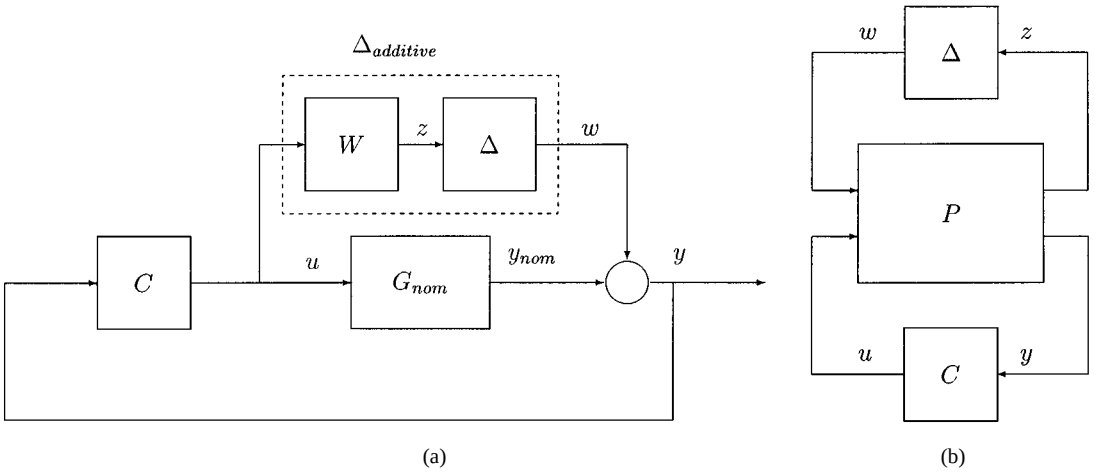

Fig. 1. (a) Additive uncertainty representation and (b) LFR of the uncertain system.

that includes the plant and the weighting functions and has the following state-space realization:

$$\begin{aligned} \dot{x} &= Ax + B_u u \\ y &= C_y x + D_{yu} u + w \\ z &= C_z x + D_{zu} u + D_{zw} w \\ w &= \Delta z, \|\Delta\|_\infty \le 1. \end{aligned} \tag{4}$$

The closed-loop system is given by

$$\begin{aligned} \dot{\tilde{x}} &= \tilde{A}\tilde{x} + \tilde{B}_w w \\ z &= \tilde{C}_z \tilde{x} + D_{zw} w \\ w &= \Delta z, \quad \|\Delta\|_\infty \le 1 \\ u &= \tilde{C}_u \tilde{x} \end{aligned} \tag{5}$$

where

$$\tilde{x} = \begin{bmatrix} x \\ x_c \end{bmatrix}, \quad \tilde{A} = \begin{bmatrix} A & B_u C_c \\ B_c C_y & A_c + B_c D_{yu} C_c \end{bmatrix}$$
$$\tilde{B}_w = \begin{bmatrix} 0 \\ B_c \end{bmatrix}, \quad \tilde{C}_z^T = \begin{bmatrix} C_z^T \\ C_c^T D_{zw}^T \end{bmatrix} \quad \text{and} \quad \tilde{C}_u^T = \begin{bmatrix} 0 \\ C_c^T \end{bmatrix}.$$

B. Performance Specifications

In order to define the specifications for the closed-loop system we define a set of initial conditions for the generalized plant in terms of a polytope $\mathcal{P}$ with vertices given by

$$x_{0,i}, \quad i = 1, 2, \ldots, n_i. \tag{6}$$

For the structural control problems these vertices can be defined to be the modal vectors that excite the individual controlled modes to desired maximum levels in the sensor outputs. With these vertices, the set $\mathcal{P}$ consists of all initial conditions that excite the structure to a sensor voltage not exceeding the prescribed maximum levels. We define a family of state trajectories $S(\tilde{x})$ of the closed-loop system in (5) in response to all initial conditions x_0 in $\mathcal{P}$ with the controller initial conditions kept zero. The specifications for the closed-loop system can now be stated as follows.

1) Robust stability to the additive uncertainty bounded by the weighting function W.
2) The closed-loop system must have a specified decay rate and maximum possible damping in all modes.
3) For every trajectory in $S(\tilde{x})$, the control input $u(t)$ satisfies

$$|u_i(t)| \le u_{\max}, \quad i = 1, 2, \ldots, n_u \tag{7}$$

where n_u is the number of control inputs.

III. Controller Design

In this section, the multiobjective controller design problem specified in the previous section will be formulated as an optimization problem involving LMIs.

A. Robust Stability

This specification involves maintaining stability of the closed-loop system in the presence of the normalized LTI uncertainty specified by (2). Following the approach in [2], the Lyapunov function for ensuring the robust stability is given by

$$V(\tilde{x}) = \tilde{x}^T X_\infty \tilde{x} + \int_0^t z(t)^T z(t)\, dt - \int_0^t w(t)^T w(t)\, dt, \quad \text{where } X_\infty = X_\infty^T > 0. \tag{8}$$

Now the robust stability problem of the closed-loop system can be formulated as a LMI feasibility problem in X_∞ as

$$\exists X_\infty = X_\infty^T > 0 \text{ such that } \begin{bmatrix} \tilde{A}^T X_\infty + X_\infty \tilde{A} & X_\infty \tilde{B}_w & \tilde{C}_z^T \\ \tilde{B}_w^T X_\infty & -I & D_{zw}^T \\ \tilde{C}_z & D_{zw} & -I \end{bmatrix} < 0. \tag{9}$$

B. Pole Placement Constraints

Using the LMI-regions [3], the condition for placing the closed-loop poles in a conic region with inner angle 2θ and a decay rate of α shown in Fig. 2 can be written as

$$\exists X_r = X_r^T \text{ such that } L_i \otimes X_r + M_i \otimes (X_r \tilde{A}) + M_i^T \otimes (\tilde{A}^T X_r) < 0, \quad i = 1, 2 \tag{10}$$

where $\otimes$ represents the Kronecker product for matrices and

$$L_1 = 2\alpha, \quad M_1 = 1$$
$$L_2 = \begin{bmatrix} 0 & 0 \\ 0 & 0 \end{bmatrix}, \quad M_2 = \begin{bmatrix} \sin\theta & \cos\theta \\ -\cos\theta & \sin\theta \end{bmatrix}. \tag{11}$$

C. Control Input Constraints

For defining the control input constraint, we consider an ellipsoid $\mathcal{E}$ given by

$$\mathcal{E} = \left\{ x \,|\, x^T X_c x \le \lambda, X_c = X_c^T > 0, \lambda > 0 \right\}. \tag{12}$$

Using the robust stability condition corresponding to the Lyapunov function in (8), the ellipsoid contains the reachable set $S(\tilde{x})$ if

$$\tilde{x}_{0,i}^T X_c \tilde{x}_{0,i} < \lambda, \quad i = 1, 2, \ldots, n_i \tag{13}$$

where $\tilde{x}_{0,i}$ is the initial condition for the closed-loop system corresponding to the vertex $x_{0,i}$ in $\mathcal{P}$ with the initial conditions for the controller being zero and n_i is the number of vertices.

The control input limit constraints can now be written as

$$\tilde{C}_{u,i}^T \lambda (u_{\max})^{-2} \tilde{C}_{u,i} < X_c, \quad i = 1, 2, \ldots, n_u \tag{14}$$

and $\tilde{C}_{u,i}$ is the row of $\tilde{C}_u$ corresponding to the ith input.

D. Multiobjective Design

With the above matrix inequality formulations of the specifications, the controller design problem can be stated as follows.

Find $X_\infty = X_\infty^T > 0$, $X_r = X_r^T > 0$, $X_c = X_c^T > 0$, A_c, B_c and C_c such that the closed-loop system satisfies the conditions given in (9), (10), (13), and (14).

But to ensure that all the specifications are satisfied simultaneously by an unique controller, it is needed that a single Lyapunov matrix to satisfy the conditions (9), (10), (13), and (14). Including this constraint, the controller design problem can be restated as follows.

Find $X = X^T > 0$, A_c, B_c and C_c such that the closed-loop system satisfies the conditions given in (9), (10), (13), and (14) with $X = X_\infty = X_r = X_c$.

E. Controller Synthesis

The conditions for the controller design given in the previous section are bilinear in the variables X, A_c, B_c, and C_c. By using a parameterization procedure [8], we convert these bilinear matrix inequalities (BLMIs) into LMIs in a different set of variables. In this parameterization, the matrix variable X is partitioned as

$$X = \begin{bmatrix} R & N \\ N^T & U \end{bmatrix} \quad \text{and} \quad X^{-1} = \begin{bmatrix} S & M \\ M^T & V \end{bmatrix} \tag{15}$$

with $R = R^T > 0$, $S = S^T > 0$ and invertible matrices M and N satisfying the relationship

$$NM^T = I - RS. \tag{16}$$

With this parameterization the controller design problem can be stated as follows.

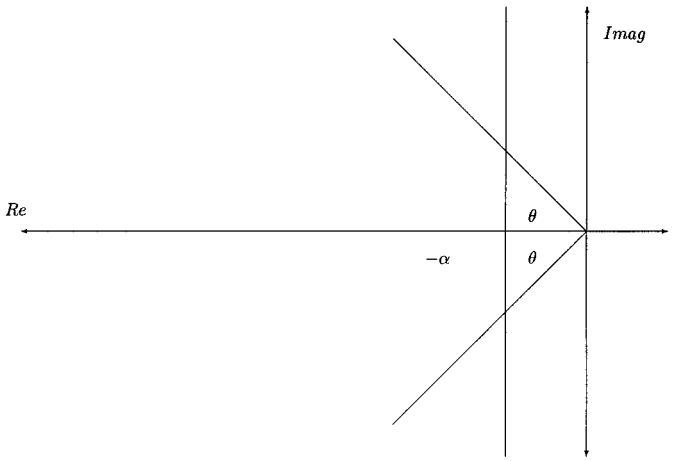

Fig. 2. LMI region.

Find $R = R^T > 0$, $S = S^T > 0$, $\lambda > 0$, A_K, B_K and C_K such that the following constraints are satisfied:

$$\begin{bmatrix} \Phi_1 + \Phi_1^T & \Phi_2 & \Phi_3 \\ \Phi_2^T & -I & D_{zw}^T \\ \Phi_3^T & D_{zw} & -I \end{bmatrix} < 0 \tag{17}$$

$$L_i \otimes \begin{bmatrix} S & I \\ I & R \end{bmatrix} + M_i \otimes \Phi_i + M_i^T \otimes \Phi_i^T < 0 \quad i = 1, 2, \ldots, n_r \tag{18}$$

$$x_{0,i}^T R x_{0,i} < \lambda, \quad i = 1, 2, \ldots, n_i \tag{19}$$

$$\begin{bmatrix} \lambda^{-1} u_{\max}^2 & C_{K,i} & 0 \\ C_{K,i}^T & S & I \\ 0 & I & R \end{bmatrix} > 0, \quad i = 1, 2, \ldots, n_u \tag{20}$$

where

$$\Phi_1 = \begin{bmatrix} AS + B_u C_K & A \\ A_K & RA + B_K C_y \end{bmatrix}$$
$$\Phi_2 = \begin{bmatrix} B_w \\ RB_w + B_K \end{bmatrix}, \quad \Phi_3 = \begin{bmatrix} SC_z^T + C_K^T D_{zu}^T \\ C_z^T \end{bmatrix} \tag{21}$$

and

$$A_K = RAS + RB_u C_K + B_K C_y S + NA_c M^T + B_K D_{yu} C_K,$$
$$B_K = NB_c \quad \text{and} \quad C_K = C_c M^T. \tag{22}$$

This problem is still nonconvex because of the presence of inverse of the variable λ in the inequalities. To enable the solution of the matrix inequalities, λ is assumed constant. An iterative search on λ is carried out until the maximum possible performance is obtained. In the following section, the formulation of the performance optimization problem is given.

F. Performance Optimization

In the specifications, it is desired that the closed-loop damping be maximized. This corresponds to placing the closed-loop poles in a conic sector shown in Fig. 2 with minimum possible inner angle 2θ. This can be formulated as a generalized eigenvalue problem (GEVP) as follows.

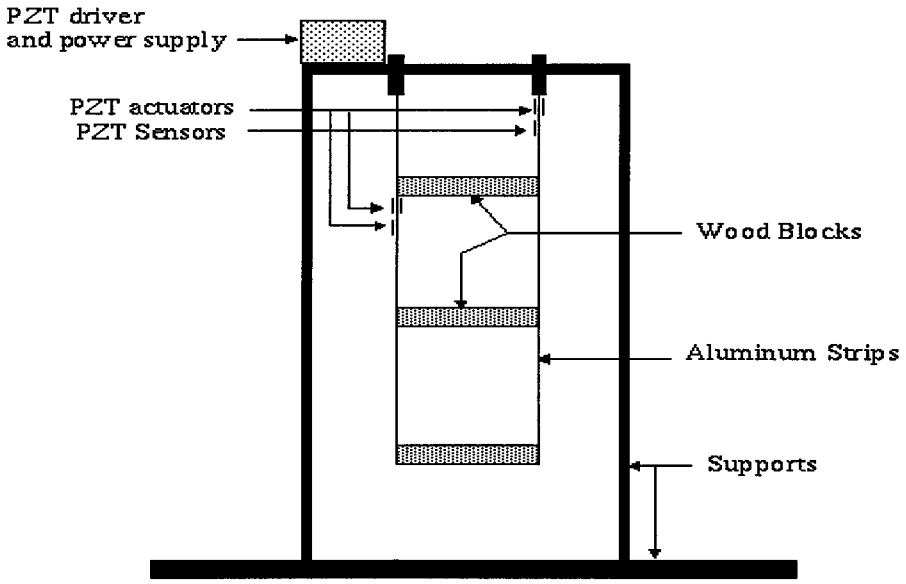

Fig. 3. Three-mass structure (two input–two output system).

Minimize γ such that

$$\begin{bmatrix} 0 & \Phi_1 - \Phi_1^T \\ (\Phi_1^T - \Phi_1) & 0 \end{bmatrix} + \gamma \begin{bmatrix} \Phi_1 + \Phi_1^T & 0 \\ 0 & \Phi_1 + \Phi_1^T \end{bmatrix} < 0 \tag{23}$$

along with other LMI constrains in (17)–(20).

The parameter γ is related to the angle θ by the following relation:

$$\gamma = \tan\theta. \tag{24}$$

The controller parameters A_c, B_c and C_c are obtained from the solution of the optimization problem, using (22) as follows:

$$A_c = N^{-1}(A_K - RAS - RB_uC_K - B_KC_yS - B_KD_{yu}C_K)M^{-T} \tag{25}$$

$$B_c = N^{-1}B_K \quad \text{and} \quad C_c = C_KM^{-T} \tag{26}$$

where M and N are obtained by performing a full rank factorization of $(I - RS)$.

IV. Results

A. System Description

For the experimental verification of the controller design procedure given in the previous sections, a 3-mass smart structure test article as shown in Fig. 3 was used. This structure consists of three blocks connected by two strips of aluminum. This 3-mass structure is mounted on a steel frame in a pendulum configuration, where the top of the structure is clamped to the frame and the bottom is left to hang free as shown in Fig. 3. In order to facilitate control of the vibrations, a pair of collocated actuators and sensors are mounted on the structure. For actuation and sensing purposes, lead zirconite titanate (PZT) ceramic patches are used. The locations of the actuators and sensors are chosen to achieve effective control of the first three modes of vibration. The control computer consists of the dSpace system, which can be used for *rapid prototyping* of real-time digital controllers. The outputs from the control computer are in the range of ± 5 V and are amplified by power amplifiers of gain 30 whose outputs drive the actuators. This translates into a limitation of ± 5 V at the input of the PZT driver power amplifier. A state-space model for the MIMO system with two actuators along with the associated conditioning circuits is obtained using swept sine frequency response measurements. The first three modes of vibration are found at 1.89, 4.86, and 7.33 Hz with each having a damping of 0.3%. For the illustration of results in this paper, a sixth-order state-space model of the structure that includes the first three modes is utilized.

B. Design Specifications

To obtain the weighting matrix corresponding to the normalized uncertainty representation initially the differences in the frequency responses of the model and experimental structure for each input output pairs are obtained. Next, the weighting function matrix W is obtained such that its minimum singular value is greater than the singular values of the frequency response error over all frequencies. The transfer function matrix for the weighting function W is given by

$$W(s) = \begin{bmatrix} 0.7 & 0 \\ 0 & 0.7 \end{bmatrix} \frac{(s+80)(s+80)}{(s+400)(s+400).} \tag{27}$$

Fig. 4 shows the comparison of the singular values of the additive uncertainty, weighting function and the nominal plant model.

For defining the control input constraints, a set of initial conditions in the form of a polytope whose vertices are the initial conditions corresponding to the modal vectors that excite the first three modes of the structural system to a maximum output of ± 0.5 V is considered.

The specifications for the control system are defined as follows.

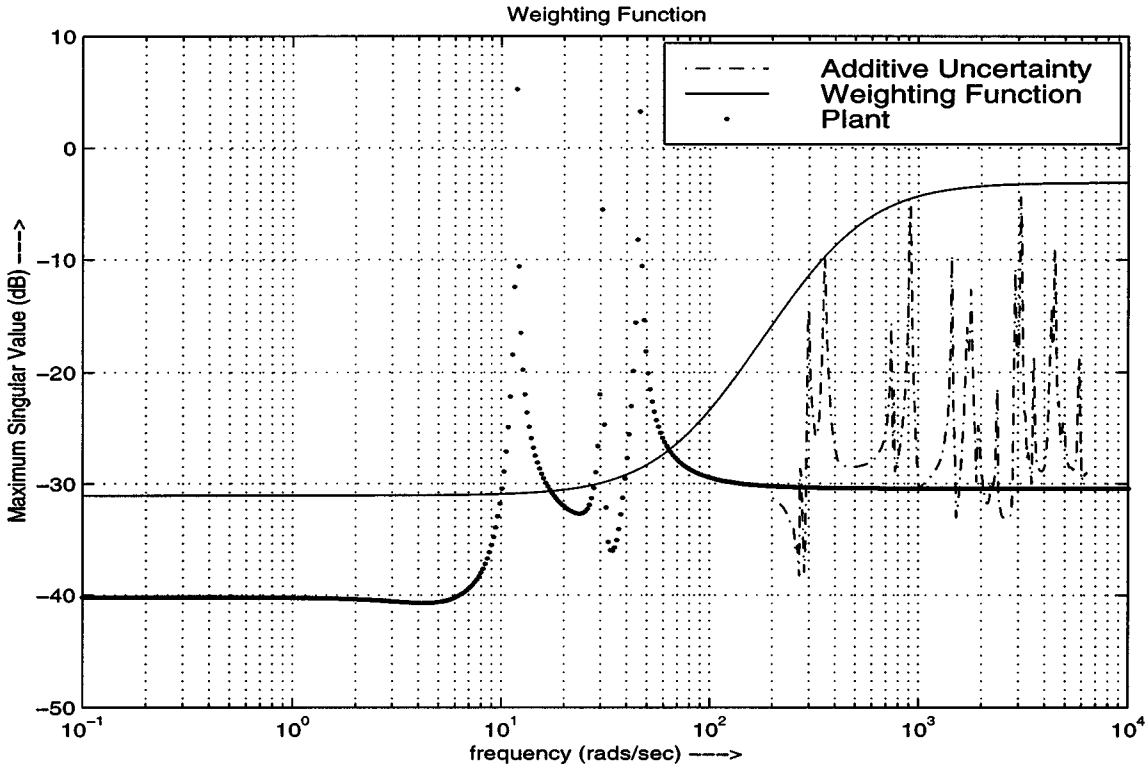

Fig. 4. Weighting function.

1) Robust stability in the presence of unmodeled dynamics: With the weighting function $W(s)$ given in (27), the robust stability requirement implies that the condition, $||T_{zw}||_\infty < 1$ be satisfied.
2) Pole placement constraints: The objective is to achieve the maximum possible decay rate α and minimum possible θ (results in an increase in damping for the closed-loop poles) in the LMI-region shown in Fig. 2.
3) Control input constraint: For the initial conditions in the polytope $\mathcal{P}$, the control input should never violate the ± 5 V limits.

C. Design and Analysis of the Controller

The generalized plant for this design is of tenth order with the nominal plant being of order 6 and the weighting function being of order 4. Hence a tenth-order controller is designed with a decay rate of $\alpha = 0.3$. Several iterations are carried out with the parameter λ until the best value is achieved. For a value of $\lambda = 3$, the best performance was achieved. The resulting decay rate was $\alpha = 0.362$ which corresponds to a damping of 3.04% in the first mode and the inner angle for the conic sector achieved was $\theta = 89.295$ degrees which corresponds to a minimum global damping of 1.01%. Fig. 5 shows the comparison of the open-loop and closed-loop poles. Note that only the poles near the imaginary axis are shown here.

To analyze the robustness of the control system we need to verify the small gain condition given by

$$||T_{zw}||_\infty < 1. \tag{28}$$

The above condition can be tested by an alternate sufficient condition given by

$$||W||_\infty ||T_{uw}||_\infty < 1 \tag{29}$$

or equivalently by

$$\sigma_{\max}(W(\omega)) < \sigma_{\min}(T_{uw}(\omega)^{-1}), \quad \forall \omega \geq 0 \tag{30}$$

where $\sigma_{\max}$ and $\sigma_{\min}$ are the maximum and minimum singular values, respectively. This requirement, though conservative, has been verified for the present problem as shown in Fig. 6. It can also be seen that the closed-loop system is actually robust to a larger set of uncertainties than the specified bound. This is a direct consequence of conservatism resulting from simultaneously satisfying multiple constraints arising from performance, control input limits and uncertainty.

To demonstrate the limitation on the achievable performance due to the inclusion of uncertainty in the design, several controllers were designed with maximum possible performance (damping) while the control input is increased in steps. Fig. 7 shows the plot of the performance against the maximum control input required. It can be seen that as the allowed control input increases, the performance increases until a point is reached after which even an increase in control input will not result in higher performance. This is due to the limitation on the achievable performance posed by the uncertainty. This point is well above the control input available for the present case, confirming the fact that the performance limitation in the present case is due to the control input limit. This also suggests that better performance can be achieved with appropriate choice of actuators.

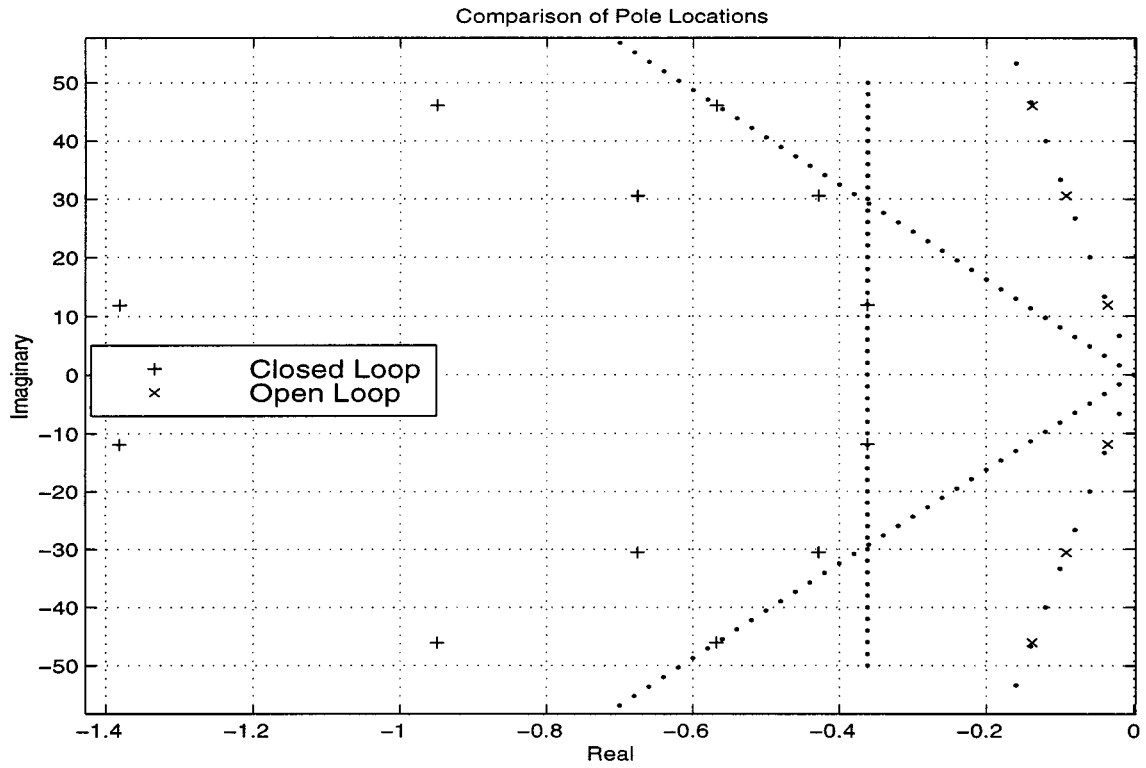

Fig. 5. Open-loop and closed-loop pole locations.

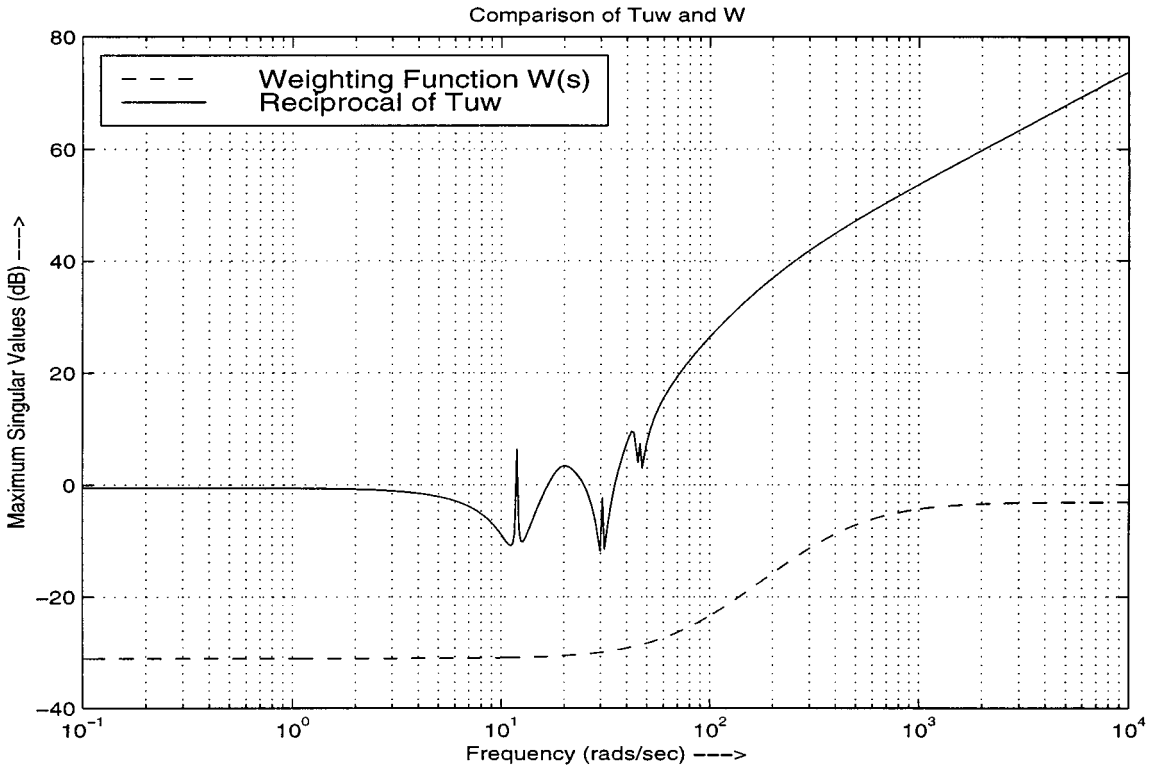

Fig. 6. Robustness analysis.

D. Controller Model Reduction

As reported in the previous section, we have designed a tenth-order output feedback controller for the experimental test article. The order of the controller can pose as a problem where ever the available hardware is small. In these cases it is required that we have a reduced order controller. This can be done by applying model reduction techniques to reduce the order of the controller. Many times, the properties of the original full-order

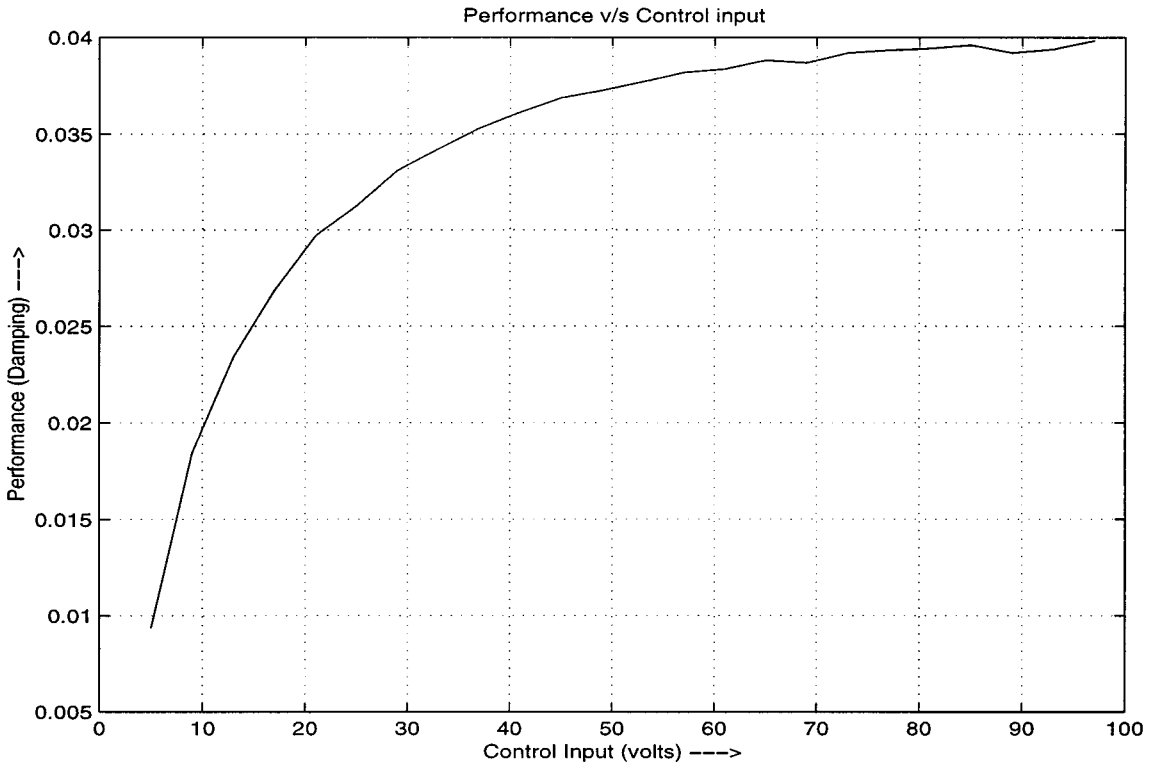

Fig. 7. Performance versus control input limit.

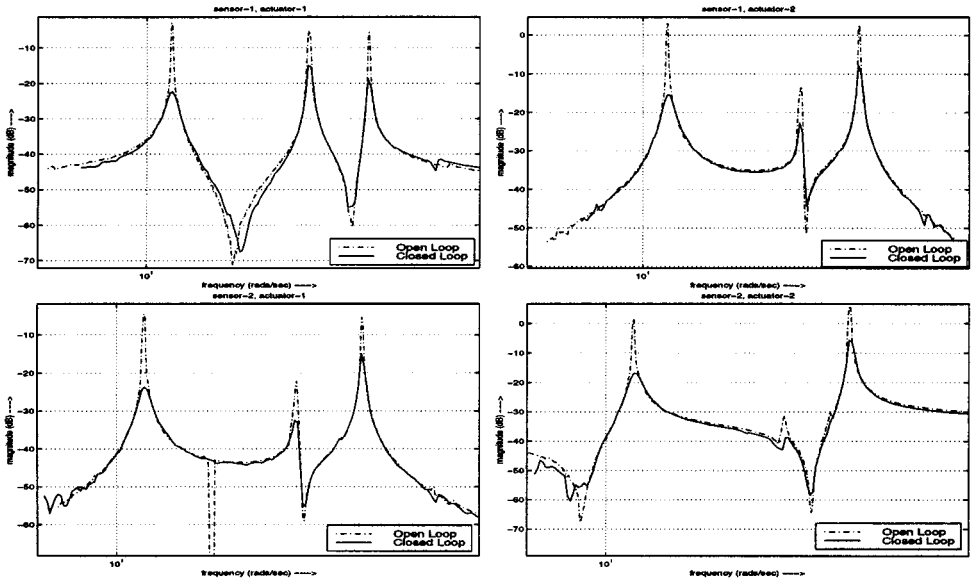

Fig. 8. Comparison of the open-loop and closed-loop frequency responses.

controller may not carry through after the application of model reduction. Hence, the reduced order controller needs to be verified for these properties before it is accepted for the application. Following this approach, a balanced model reduction was carried out on the full-order controller and a sixth-order controller that satisfied all the robustness and performance specifications was found. The comparison of the singular values of the full-order and the reduced order controllers revealed that they are indistinguishably identical in the frequency range of interest. Hence, the reduced order controller is used for all the following experimental results and analysis.

E. Experimental Results

In order to show the effectiveness of the controller, the measurements of the frequency response of the closed loop system were carried out. Fig. 8 shows the comparison of the frequency responses for the open-loop with the closed-loop control system.

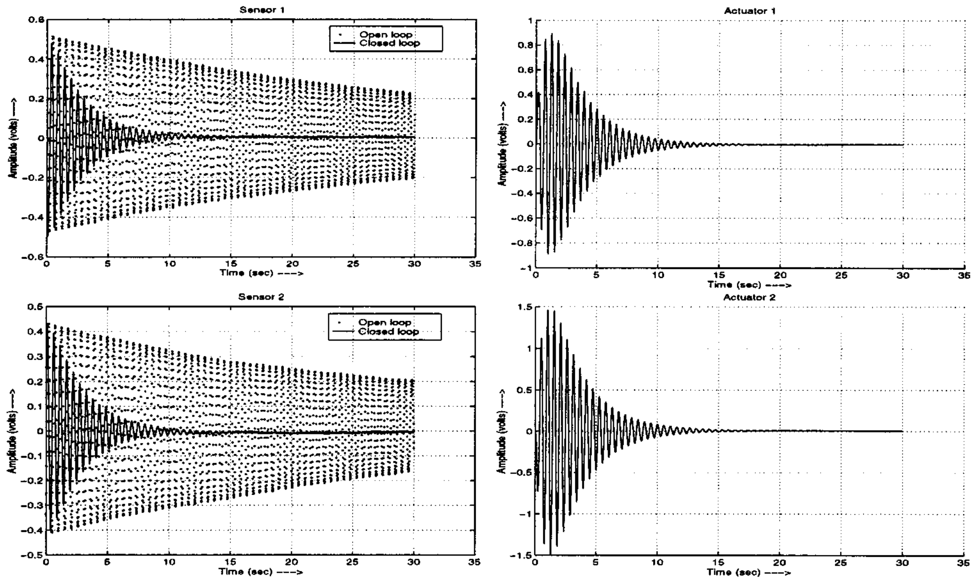

Fig. 9. Controller performance (first mode).

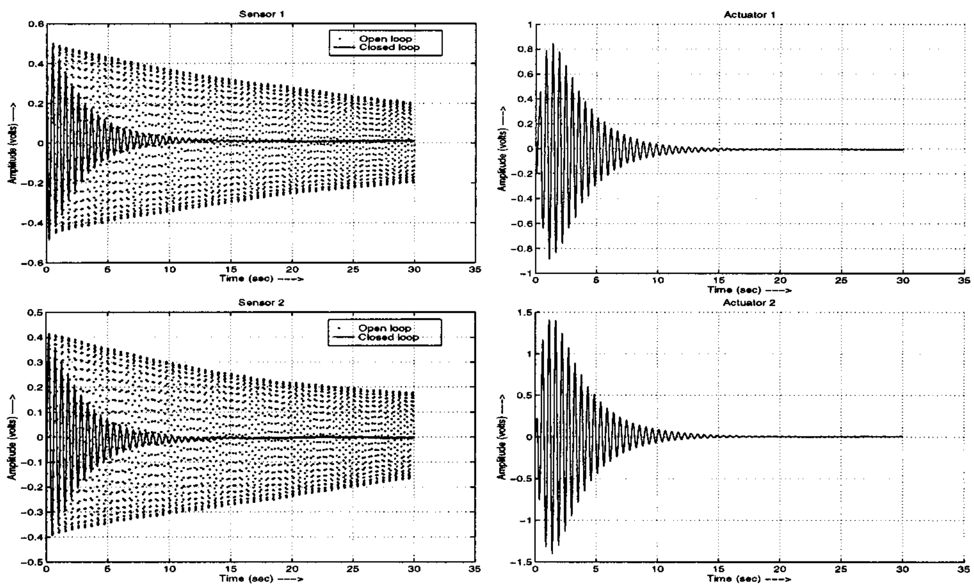

Fig. 10. Robustness verification.

It can be seen that the damping of the modes has been considerably increased. The achieved damping for the first mode is larger than the global damping because of the use of a decay rate of $\alpha = 0.3$ in the design.

To show the performance of the control system, the specified initial conditions are generated by exciting the structure to a level of ±0.5 V in the sensor outputs for the modes considered in the nominal plant. At steady state, the excitation is withdrawn and the controller is switched on. The results of the controller performance for the initial conditions corresponding to the first mode are shown in Fig. 9. From these results, it can be concluded that the system has good damping and the control inputs were always within the specified limits. To test the robustness features of the control system, a signal corresponding to an higher order mode in the unmodeled dynamics at frequency 147.2 Hz with an initial condition amplitude of ±0.1 V is applied in addition to the initial condition excitation of ±0.5 V in the first mode. The comparison of the open-loop and closed-loop responses of the control system is shown in Fig. 10. From these figures it can be seen that the closed-loop system performance is unchanged. The control input limits were also within the specified limits. This test showed that the control system is robust to unmodeled dynamics and hence is devoid of spill-over problems.

V. Conclusion

An output feedback robust controller design problem is formulated for smart structural systems with control input limits to eliminate spill-over problems. The method is tested on an experimental smart structure and the robustness of the control system is demonstrated. Because of the inclusion of the control

input limits and robustness conditions in the design procedure, it allows one to concentrate on achieving the maximum possible performance without worrying about violation of any of these constraints. Conservatism in the design can be reduced by proper choice of the parameter λ. Because, this parameter appears in a nonconvex manner, direct optimization is not possible. Investigation of conversion of this nonconvex problem into an equivalent convex problem is currently underway. The order of the controller resulting from the present procedure is the sum of the order of the plant dynamics and the order of the weighting function. A reduced order controller which matches the full-order controller performance has been implemented on the test article. In future research, the design procedure will be extended to develop lower order controllers instead of using model order reduction.

REFERENCES

[1] M. J. Balas, "Trends in large space structures control theory: Fondest hopes, wildest dreams," *IEEE Trans. Automat. Contr.*, vol. AC-27, pp. 522–535, June 1982.

[2] S. Boyd, L. El Ghaoui, E. Feron, and V. Balakrishnan, *Linear Matrix Inequalities in Systems and Control Theory*, vol. 15 of Studies in Applied Mathematics, 1994.

[3] M. Chilali and P. Gahinet, "Design with pole placement constraints: An LMI approach," *IEEE Trans. Automat. Contr.*, vol. 41, pp. 358–367, Mar. 1996.

[4] P. Gahinet, A. Nemirovski, and A. J. Laub, *LMI Control Toolbox: User's Guide*. Natick, MA: The MathWorks, Inc., 1995.

[5] Y. Nesterov and A. Nemirovski, *Interior Point Polynomial Methods in Convex Programming: Theory and Applications*. Philadelphia, PA: SIAM, 1994.

[6] A. Packard *et al.*, "A collection of robust control problems leading to LMI's," in *Proc. IEEE Conf. Decision Contr. '91*, 1991, p. 1245.

[7] S. Sana and V. Rao, "Robust control of input limited smart structural systems," presented at the 6th Annu. Int. Symp. Smart Struct. Materials, Newport Beach, CA, 1999.

[8] C. Scherer, P. Gahinet, and M. Chilali, "Multiobjective output-feedback control via LMI optimization," *IEEE Trans. Automat. Contr.*, vol. 42, pp. 896–911, July 1997.

[9] K. Zhou, J. C. Doyle, and K. Glover, *Robust and Optimal Control*. Englewood Cliffs, NJ: Prentice-Hall, 1996.

[10] L. El Ghaoui and G. Scorletti, "Control of rational systems using linear fractional representations and linear matrix inequalities," *Automatica*, vol. 32, no. 9, pp. 1273–1284, 1996.